J Low Temp Phys
DOI 10.1007/s10909-014-1255-9

Influence of the Fe Concentration on the Superconducting Properties of $Fe_{1-y}Se$

M. L. Amigó · M. V. Ale Crivillero · D. G. Franco · J. Guimpel · G. Nieva

Received: 16 August 2014 / Accepted: 18 November 2014
© Springer Science+Business Media New York 2014

Abstract We present a comparative study of electrical transport properties in the normal state and in the dissipative superconducting state between pure β-FeSe phase and Fe deficient $Fe_{1-y}Se$ crystals. We discuss the influence of the intergrowth of the magnetic hexagonal phase (Fe_7Se_8) in Fe deficient samples when compared to pure β-FeSe samples. In the superconducting state, we measured the *ab*-plane electrical resistivity with magnetic field up to 16 T and the electrical resistivity as a function of the angle between the *c* axis and the applied field. The angular dependence at fixed temperature below the superconducting critical temperature, $T_c(H = 0)$, is very different for both sets of crystals. The Fe deficient samples display a vortex pinning-related feature at $\sim 57°$ off the plane while the pure β-FeSe phase samples show the persistence of a strong angular-dependent magnetoresistance characteristic of the normal state electronic structure.

Keywords Chalcogenide · Vortex pinning · Correlated defects · Electrical transport · Fe deficiency

1 Introduction

FeSe is a member of the widely studied family of Fe-based superconductors. Many of the physical properties of this material were found to be strongly dependent on the

M. L. Amigó · M. V. Ale Crivillero (✉) · D. G. Franco · J. Guimpel · G. Nieva
Comisión Nacional de Energía Atómica, Centro Atómico Bariloche and CONICET, S.C. de Bariloche, Río Negro, Argentina
e-mail: victoria.ale@ib.edu.ar

G. Nieva
e-mail: gnieva@cab.cnea.gov.ar

M. L. Amigó · M. V. Ale Crivillero · D. G. Franco · J. Guimpel · G. Nieva
Instituto Balseiro and Universidad Nacional de Cuyo, S.C. de Bariloche, Río Negro, Argentina

Published online: 04 December 2014

Fe concentration. The superconducting β-FeSe phase is difficult to obtain in pure single crystalline form given its very narrow range of existence in the thermodynamic phase diagram [1]. The Fe content in crystals produced with different methods indicates the phases intergrown with the superconducting β-FeSe, typically Fe excess indicates the presence of metallic Fe, and Fe defect the presence of ferrimagnetic γ-Fe_7Se_8. The mix of phases is possibly responsible for diverse behaviors reported in the literature for FeSe. Some authors observed that only samples near perfect stoichiometry display the highest transition temperatures [2]. Others that disorder and impurity phases enhance the superconducting properties [3]. In this work we present the growth and characterization of pure β-FeSe and Fe deficient mixed β-FeSe and γ-Fe_7Se_8 single crystals, and a preliminary experimental study of their electrical transport properties in the normal and superconducting state.

2 Crystal characterization

$Fe_{1-y}Se$ single crystals were grown using two variants of the flux method. In one case, the flux composition was $\frac{1}{4}$KCl:$\frac{3}{4}$NaCl and the material encapsulated in a quartz ampoule was ramped in temperature up to a maximum of $T = 850°C$. Then an annealing at a constant temperature of 700°C for 4 days was carried out. In the second case, the flux is KCl: $2AlCl_3$ and the ampoule was placed at a temperature gradient [4] with the hot part at 395°C and the cold part at 385°C for 45 days. Throughout this manuscript, samples A and A1 are crystals grown with the first method and sample B is a crystal grown with the second method. The flux's melting point determined the temperature range for the growth [5,6]. The lower temperature of the second method allows us to grow the crystals in the desired phase avoiding high temperature structural phase transitions and decompositions [1].

We use X-ray diffraction (XRD) and Energy Dispersive Spectroscopy to characterize the crystal structure and composition. Crystals from both methods have a platelet shape. While both crystals show Fe deficiency, the deficiency is smaller for crystal B, $y = 0.04$ ($Fe_{0.96}Se$), than for crystal A, $y = 0.08$ ($Fe_{0.92}Se$). XRD indicates the presence of superconducting β-FeSe and ferrimagnetic hexagonal γ-Fe_7Se_8, in crystal A. For the superconducting phase, the $(l0l)$ and $(l00)$ directions are perpendicular to the crystal surface, while the hexagonal phase grows with the ab-plane parallel to the surface [7]. In crystal B, only the tetragonal superconducting β-FeSe phase with the c axis perpendicular to the crystal surface is present as identified by room temperature XRD. The lattice parameters of the superconducting phase are $a = (3.78 \pm 0.03)\mathring{A}$, $c = (5.51 \pm 0.03)\mathring{A}$ for crystal A and $a = (3.77 \pm 0.01)\mathring{A}$ and $c = (5.52 \pm 0.01)\mathring{A}$ for crystal B.

3 Results and discussion

Figure 1a and b show the temperature dependence of the in plane resistivity for the normal state of samples A and B without and with a 16T applied magnetic field perpendicular to the platelet plane. Data were acquired in a standard 4 probe con-

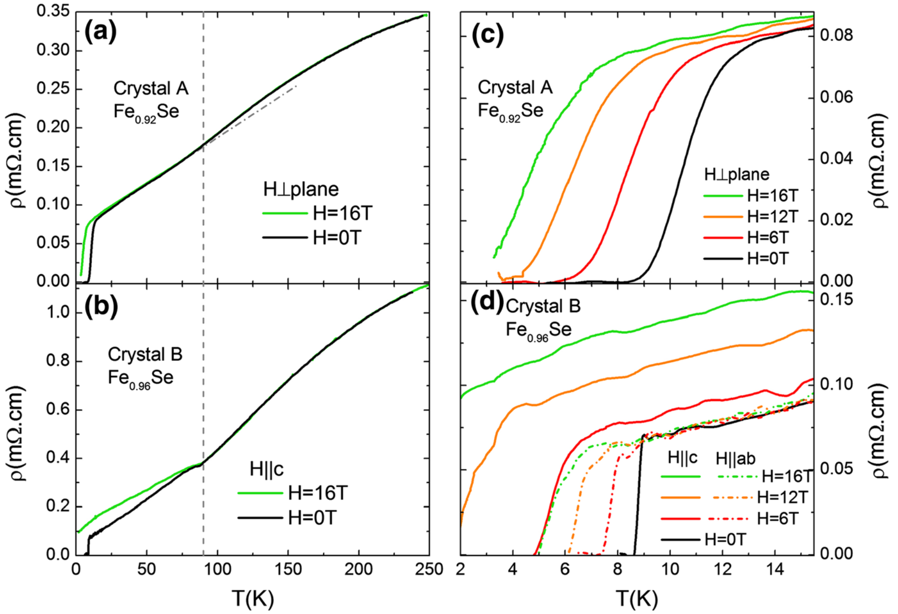

Fig. 1 Temperature dependence of the in plane resistivity for **a** crystal A ($Fe_{0.92}Se$) and **b** crystal B ($Fe_{0.96}Se$) with an applied magnetic field of $H = 0$ and 16 T perpendicular to the crystal plane ($H \perp$ plane). The *dashed line* points out the temperature of the structural transition [8]. The *dash-dotted line* shows the change in the slope for crystal A. **c** and **d** Detail of the superconducting transition with and applied magnetic field of $H = 0$, 6, 12 and 16 T, for crystals A and B, respectively (Color figure online)

tact configuration. Both crystals present similar characteristics, the resistivity has a metallic-like behavior at high temperatures and at $T \sim 90$ K there is a change in slope, more pronounced for sample B. At this temperature a structural transition from the tetragonal to an orthorhombic phase is found [8]. The temperature dependence of the magnetization shows a contribution of the ferrimagnetic Fe_7Se_8 for crystal A [7], but there is no evidence of a magnetic feature at the structural transition temperature for either sample. Although the temperature dependence of the resistivity for both crystals is very similar, there is a difference in its value. Sample A has a value similar to that of pure Fe_7Se_8, lower than that for sample B. Below 90 K, crystal B presents a positive magnetoresistance for the field parallel to the *c* axis, and a negligible magnetoresistance for the field in the *ab*-plane, see Fig. 1b and d. The magnetoresistance could be explained taking into account an anisotropic multiband behavior [9]. Its emergence at the structural transition may be a signature of a change in the electronic structure [10]. No measurable magnetoresistance, in the same temperature range, was observed in crystal A as reported in other crystals with phase coexistence [11]. However, a behavior similar to that of crystal B has been reported in films [12] and polycrystals [13]. For sample B, magnetic field parallel or perpendicular to the crystal surface, implies magnetic field aligned to the *ab*-plane or to the *c* axis, respectively. On the contrary, in crystal A, when the field is perpendicular to the platelet plane, it is neither in the *c* axis nor in the *ab*-plane. The coexistence of phases and crystalline directions could average the anisotropic angular dependence of the magnetoresistance, but the reason

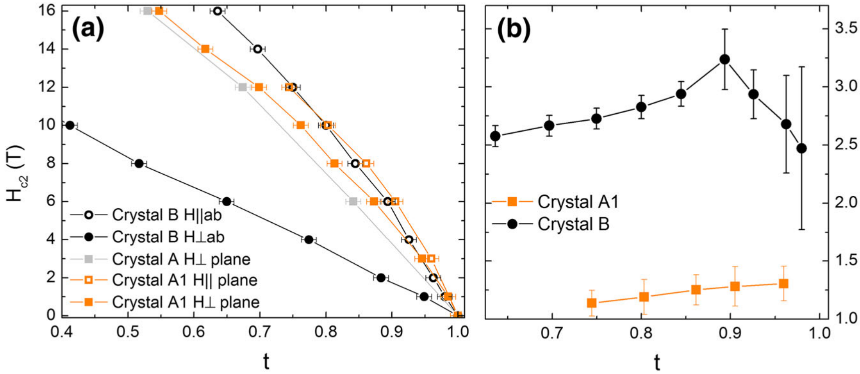

Fig. 2 **a** Critical magnetic field H_{c2} as a function of the reduced temperature ($t = T/T_c(H = 0)$) for crystals A, A1 and B for the field in the crystal plane ($H \parallel$ plane) and perpendicular ($H \perp$ plane) to it. **b** Anisotropy ($\gamma = H_{c2\parallel}/H_{c2\perp}$) for crystals A1 and B (Color figure online)

for the negligible absolute value of the magnetoresistance in A-type samples is not clear to us and may be of a more microscopic electronic nature.

In order to study the superconducting state for crystals A and B, we measured the temperature dependence of the in-plane resistivity with an applied magnetic field, see Fig. 1c and d. In both samples, the transition width increases with field. This signals the possibility of a narrow region with a vortex liquid phase. The transition temperatures for $H = 0$ are $T_c = (12.0 \pm 0.1)$ K and $T_c = (8.87 \pm 0.05)$ K for crystals A and B, respectively, which is a remarkable difference. The crystal with a lower Fe content and coexistence of phases has a higher T_c. About this point, there is no agreement in the literature [2,14,15]. The T_c of FeSe is very sensitive to the external pressure [16], but there is no difference in the lattice parameter of the samples to justify an internal pressure produced by the Fe vacancies.

Figure 2a shows the temperature dependence of the parallel and perpendicular critical magnetic field, $H_{c2}(T)$, for samples A, A1, and B, defined as the onset of the transition from the curves in Fig. 1c, d. A detailed study of $H_{c2}(T)$ for B-type samples was performed in ref. 9. The values of $H_{c2}(T)$ for crystal A and A1 are in between those for sample B. Therefore, crystal B presents a more anisotropic behavior, see Fig. 2b. A shared characteristic for both types of sample is the decrease at low temperatures of the anisotropy ($\gamma = H_{c2\parallel}/H_{c2\perp}$). This is an indication of a multiband behavior [9].

To study the influence of the coexistence of phases and possible correlated defects in the superconducting state, we measured the resistivity as a function of the angle, θ, between the applied magnetic field and the normal to the crystal plane, see Fig. 3a and b. In the case of crystal B, $H = 16$ T and $T = (5.12 \pm 0.01)$ K, there is only a narrow angular range, near 90°, in which the sample is in the superconducting state. Out of this narrow range, the angular dependence is the same as that of the magnetoresistance in the normal state, as can be seen for $H = 16$ T and $T = (8.12 \pm 0.01)$ K. This dependence, as well as the magnetoresistance, becomes negligible above the structural transition at 90 K.

For crystal A, at $H = 16$ T and $T = (4.94 \pm 0.04)$ K, the sample is below H_{c2} for all field directions. In the vortex state of an anisotropic superconductor, a monotonous

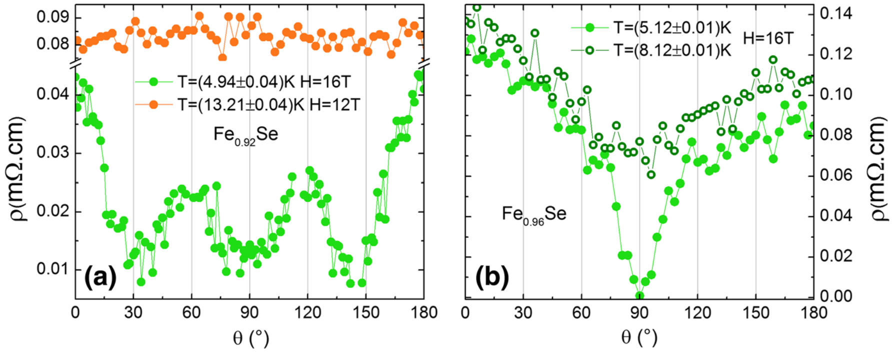

Fig. 3 Resistivity as a function of the angle between the normal to the surface and the applied magnetic field, for crystals A and B, **a** and **b** panels, respectively. Two fixed temperatures were chosen, below and above T_c (Color figure online)

angular behavior of the resistivity is expected [17], with a minimum when the field is parallel to the *ab*-plane and a maximum for the field in the *c* axis. This does not completely explain the angular dependence of sample A, because there are two extra minima at ∼33° and ∼147°. The depth of the minima varies between crystals of the A-type, but they are present in all measured samples. The angles 33° and 147° correspond to the direction of the *ab*-plane considering that the $(l0l)$ plane is parallel to the crystal surface. We find two possible scenarios for the origin of the extra minima. The first one depends on the coexistence of crystalline phases. The matching interface between β-FeSe and Fe_7Se_8 is achieved matching the β-FeSe (101) plane to the Fe_7Se_8 plane with high density of vacancies. This interface could act as a correlated defect at ∼33° [18]. The second scenario consists in considering that, according to the XRD results, there are three coexistent orientations of the *ab* plane, ∼33°, ∼90° and ∼147°. For $H \parallel ab$ in each orientation, the angular dependence of the resistivity for the β-FeSe phase presents a minimum, given the higher $T_c(H)$ for this crystallographic direction. The resistivity in crystal A in this scenario is either a series or parallel combination of the three angular dependencies with the minima located at θ= 33°, 90° and 147°. Above T_c, the absence of angular dependence on the resistivity is consistent with this picture. However, this phenomenological model predicts a positive magnetoresistance in the normal state which is not experimentally observed. This will be further discussed elsewhere [7,9].

4 Conclusions

With two variants of the flux method, we obtain single crystals of pure β-FeSe and Fe deficient $Fe_{1-y}Se$ (β-FeSe + Fe_7Se_8). Both types of crystal present a structural transition, which is observable in resistivity measurements. Below this transition temperature, the crystals of β-FeSe present a positive anisotropic magnetoresistance which could be related to a multiband behavior. The absence of magnetoresistance in $Fe_{1-y}Se$ is puzzling and cannot be explained by a simple model of parallel or series combination of the intermixed phases, implying that a more microscopical approach is needed.

In the superconducting state, the angular dependence of the dissipation at fixed temperature and field is very different for both crystals. The Fe deficient samples display a vortex pinning-related feature at $\sim 57^\circ$ off the plane while the pure β-FeSe phase samples show the persistence of a strong angular-dependent magnetoresistance characteristic of the normal state electronic structure.

Acknowledgments We thank F. Gennari for help in sample preparation. We thank Conicet PIP1122009010 0448 and Sectyp U. N. Cuyo for financial support.

References

1. H. Okamoto, J. Phase Equilib. **12**(3), 383 (1991)
2. Sudesh, S. Rani, S. Das, R. Rawat, C. Bernhard, G.D. Varma, J. Appl. Phys. **111**, 07E119 (2012)
3. A. Wittlin, P. Aleshkevych, H. Przybylińska, D.J. Gawryluk, P. Dłużewski, M. Berkowski, R. Puźniak, M.U. Gutowska, A. Wiśniewski, Supercond. Sci. Technol. **25**(6), 065019 (2012)
4. D. Chareev, E. Osadchii, T. Kuzmicheva, J.Y. Lin, S. Kuzmichev, O. Volkova, A. Vasiliev, Cryst. Eng. Commun. **15**(10), 1989 (2013)
5. D.S. Coleman, P.D.A. Lacy, Mater. Res. Bull. **2**, 935 (1967)
6. C. Robelin, P. Chartrand, A.D. Pelton, J. Chem. Thermodyn. **36**, 683 (2004)
7. M.L. Amigó, M.V. Ale Crivillero, D.G. Franco, A. Badía Majóz, J. Guimpel, G. Nieva. to be published
8. T.M. McQueen, A.J. Williams, P.W. Stephens, J. Tao, Y. Zhu, V. Ksenofontov, F. Casper, C. Felser, R.J. Cava, Phys. Rev. Lett. **103**(5), 057002 (2009)
9. M.L. Amigó, V. Ale Crivillero, D.G. Franco, G. Nieva; arXiv:1411.3664v1
10. T. Shimojima, Y. Suzuki, T. Sonobe, A. Nakamura, M. Sakano, J. Omachi, K. Yoshioka, M. Kuwata-Gonokami, K. Ono, H. Kumigashira, A.E. Böhmer, F. Hardy, T. Wolf, C. Meingast, H.v. Löhneysen, H. Ikeda, K. Ishizaka, Phys. Rev. B **90**(12), 121111 (2014)
11. U. Patel, J. Hua, S.H. Yu, S. Avci, Z.L. Xiao, H. Claus, J. Schlueter, V.V. Vlasko-Vlasov, U. Welp, W.K. Kwok, Appl. Phys. Lett. **94**, 082508 (2009)
12. H.H. Chang, J.Y. Luo, C.T. Wu, F.C. Hsu, T.W. Huang, P.M. Wu, M.K. Wu, M.J. Wang, Supercond. Sci. Technol. **25**, 035004 (2012)
13. H. Chu, J. Li, S. Li, Y. Zhang, N. Wang, J. Wang, Y. Gao, H. Deng, X. Sun, D. Zheng, Sci. China: Phys., Mech. Astron. **53**, 1180 (2010)
14. T.-K. Chena, C.-C. Changa, H.-H. Changb, A.-H. Fanga, C.-H. Wanga, W.-H. Chaoa, C.-M. Tsenga, Y.-C. Leea, Y.-R. Wua, M.-H. Wena, H.-Y. Tangd, F.-R. Chena, M.-J. Wanga, M.-K. Wua, D. Van Dycke, PNAS **11**(1), 63 (2014)
15. M. Bendele, P. Babkevich, S. Katrych, S.N. Gvasaliya, E. Pomjakushina, K. Conder, B. Roessli, A.T. Boothroyd, R. Khasanov, H. Keller, Phys. Rev. B **82**, 212504 (2010)
16. D. Braithwaite, B. Salce, G. Lapertot, F. Bourdarot, C. Marin, D. Aoki, M. Hanfland, J. Phys.: Condens. Matter **21**, 232202 (2009)
17. G. Blatter, M.V. Feigel'man, V.B. Geshkenbein, A.I. Larkin, V.M. Vinokur, Rev. Mod. Phys. **66**(4), 1125 (1994)
18. M.L. Amigó, V. Ale Crivillero, D.G. Franco, A. Badía-Majós, J. Guimpel, G. Nieva. J. Phys.: Conf. Ser. **507**, 012001 (2014)